American Mineralogist, Volume 64, pages 748–757, 1979

Armangite, $Mn_{26}^{2+}[As_6^{3+}(OH)_4O_{14}][As_6^{3+}O_{18}]_2[CO_3]$, a fluorite derivative structure

PAUL B. MOORE AND TAKAHARU ARAKI

Department of the Geophysical Sciences, The University of Chicago
Chicago, Illinois 60637

Abstract

Armangite, $Mn_{26}^{2+}[As_6^{3+}(OH)_4O_{14}][As_6^{3+}O_{18}]_2[CO_3]$, $a_1 = 13.491(2)$, $c = 8.855(1)$A, $Z = 1$, $P\bar{3}$, was studied in detail by three-dimensional X-ray diffractometry. $R = 0.072$ ($R_w = 0.056$) for all 4012 non-equivalent reflections, and $R = 0.043$ for 2749 observable reflections above three times background error. X-ray diffraction data to $\sin\theta/\lambda = 0.80$ (Mo$K\alpha$ radiation, graphite monochromator) were collected on a Picker four-circle diffractometer, and the structure was solved by Patterson, Fourier, difference synthesis, and least-squares refinement techniques. The $[CO_3]$ group was located on a difference synthesis, confirmed by electron probe analysis on select pure grains.

The structure is an anion-deficient fluorite derivative structure where a_1 (arm) $= 2\sqrt{2}\ a_1$ (flu) and c (arm) $= \sqrt{3}\ a_1$ (flu) corresponding to a 4.94A fluorite average edge. The fluorite stoichiometry is $X_{48}\phi_{96}$, where $48X = 26Mn^{2+} + 18As^{3+} + 1(CO_3) + 3\square(1)$, the cation vacancies occurring at ½ ½ 0, *etc.*; and $96\phi = 54$ O(1) through O(9) + 42□(a) through □(i). Bond distance averages are $^{[3]}$C–O 1.30, $^{[3]}$As(1)–O 1.78, $^{[3]}$As(2)–O 1.78, $^{[3]}$As(3)–O 1.79, $^{[6]}$Mn(1)–O 2.21, $^{[6]}$Mn(2)–O 2.22, $^{[6]}$Mn(3)–O 2.22, $^{[6]}$Mn(4)–O 2.24, and $^{[6]}$Mn(5)–O 2.22A. The (CO_3) groups are disordered so O(10) is on the average only half-occupied. A cluster of composition $Mn_6^{2+}As_6^{3+}C^{4+}O_{33}$ can be extracted which is related to the arrangement in the Fe^{3+} oxyphosphate sheet of mitridatite, which also locally is a fluorite derivative structure. Mn(1), Mn(2), Mn(3), and Mn(5) are distorted octahedra, Mn(4) is a distorted trigonal prism, and As(1), As(2), and As(3) are distorted trigonal pyramids. Local environments in armangite are similar to those in magnussonite, a related structure, but central Mn^+ in armangite is missing.

Introduction

Armangite, originally described by Aminoff and Mauzelius (1920), occurred as a rare late-stage mineral in basic, reduced veins with calcite and barite from Langban, Sweden. These authors interpreted the original analysis as including the presence of an admixed carbonate, and deduction of these impurities led to the relatively simple composition $Mn_3^{2+}(AsO_3)_2$. Despite the simple composition the cell contains nine formula units, and question arose regarding the possible space groups (originally listed as rhombohedral) despite the trigonal development of the crystals. Our study shows that the extinction criteria definitely belong to a trigonal group, specifically $P\bar{3}$, and that the compound does not possess such a simple composition.

Work on armangite's structure was initiated by the senior author ten years ago, but the problem was abandoned owing to its inherent difficulty. Not until our study on the compositionally-related magnussonite (Moore and Araki, 1979) did we discover a relationship between these phases and the relatively simple and versatile fluorite structure type. This relationship, coupled with the presence of arsenite groups which include lone pair electrons, revitalized our interest in the problem.

Experimental section

A small fragment of Flink unknown U71 (from the Swedish Natural History Museum) showed pale brown hexagonal prisms embedded in dolomite–hausmannite rock. It was investigated fourteen years ago and shown to be identical with armangite through single-crystal X-ray and powder photography. More recently, a fragment of specimen R5795 (National Museum of Natural History, Smithsonian

0003–004X/79/0708–0748$02.00

Table 1. Armangite: chemical data

	1	1a	2	3
MnO	45.06	47.06	51.82	49.78
FeO	2.19	2.49	-----	-----
PbO	0.32	0.36	-----	-----
CaO	2.83	-----	-----	-----
MgO	0.49	-----	-----	-----
As_2O_3	42.92	48.82	48.18	48.06
Sb_2O_3	0.40	0.46	-----	-----
CO_2	5.08	-----	-----	1.19
H_2O	0.71	0.81	-----	0.97
Insol.	0.20	-----	-----	-----
Total	100.20	100.00	100.00	100.00

[1]Mauzelius analysis in Aminoff and Mauzelius (1920).

[1a]Recalculated after deduction of insol., CO_2, CaO, MgO and MnO (3.69%) as $(Ca,Mn,Mg)CO_3$. See Palache et al. (1960) from which this was copied.

[2]For $Mn_3^{2+}(AsO_3)_2$.

[3]For $Mn_6^{2+}[As_6^{3+}(OH)_4O_{14}][As_6^{3+}O_{18}](CO_3)$. The calculated density is $\rho = 4.406$ g cm^{-3}. The specific gravity is 4.43 (Palache et al., 1960).

Institution) showing coarse hexagonal crystals was examined in detail by single-crystal study; the results agreed in every respect with the U71 sample. This specimen was a cotype originally studied by Aminoff, who named and described the mineral (Aminoff and Mauzelius, 1920).

Two data sets were collected on fragments from U71. The first was a prismatic fragment which presented Laue class $\bar{3}$ $2/m1$, and three-dimensional data were collected on a Pailred linear diffractometer. A trial structure determination proceeded from Patterson synthesis, $P(uvw)$, but the solution met failure. A comprehensive program for twinned crystals (Araki, 1977) revealed that merohedral twinning on (110) for space group $P\bar{3}$ gave the desired results. Crude atomic positions were then obtained in this fashion.

Search for an untwinned crystal led to a second reflection data set on a Picker four-circle diffractometer, with the ϕ-axis || c. From the orientation matrix, the cell constants were refined to $a = 13.491(2)$, $c = 8.855(1)$A. Salient details: crystal size 0.086 × 0.060 × 0.25 (||c) mm, Mo$K\alpha$ radiation with graphite monochromator, 1° min^{-1} scan speed, 1.6° scan width, 20 sec background counting times on both sides of the scan, maximum $\sin\theta/\lambda = 0.80$. Two equivalent reciprocal spaces were covered, $h \leqq 0$, $k \geqq 0$, $l \geqq 0$ and $h \geqq 0$, $k \leqq 0$, $l \geqq 0$. Unobserved reflections with $I_o < 2\sigma(I)$ were reset as $I_o(hkl) = \sigma(I)$. A total of 442 reflections fell into this category. Absorption correction by the Gaussian integral method (Burnham, 1966) employed 11 faces and 7 divisions with $u_a = 166.6$ cm^{-1} for linear absorption coefficient. (After knowledge of the structure we calculated $u_a = 172.1$ cm^{-1}, but this difference is small and is within the error range of the crystal size measurement.) Inspection of the anisotropic thermal vibration ellipsoids (Table 4), indeed, indicated that any absorption anisotropy is minimal. The absorption correction was substantial owing to the crystal shape, which yielded transmission factors between 0.089 and 0.224. After correction, equivalent reflections were inspected, found satisfactory, and averaged to obtain 4012 independent $|F_o|$.

The structure analysis indicated the presence of $(CO_3)^{2-}$ groups in the structure. Accordingly, we separated a clear grain which was polished and gold-coated for electron-probe analysis using 5 kV and 700 nA beam current. With counts in multiples of 10 sec and pyrolytic graphite as a standard, the data were extrapolated to zero time and yielded 0.9±0.2 percent C with carbon counts about three times above background. This result confirms the presence of $(CO_3)^{2-}$ groups in the structure of armangite and shows (Table 1) that not all CO_2 reported in Aminoff and Mauzelius (1920) was due to admixed carbonate. Furthermore, the complex structure of armangite is in part due to the presence of carbonate groups in small amount, which yields a large cell, not expected for a relatively simple composition such as $Mn_3^{2+}(AsO_3)_2$! The presence of hydroxyl groups in armangite's structure also confirms the small amount of H_2O reported in the Mauzelius analysis. Indeed, inspection of broken armangite crystals showed thin films of carbonate coatings. Thus, wet-chemical analysis of armangite must have presented special problems.

Structure determination and refinement

Programs used in determining and refining the structure were listed earlier (Moore and Araki, 1976a). Crude atomic positions were obtained from the Patterson synthesis on the first data set. The superior data were then utilized toward further refinement. Scattering curves for Mn^{2+}, As, O^- and C were obtained from Ibers and Hamilton (1974, p. 99–100).

Table 2. Armangite: atomic coordinate parameters†

Atom			x	y	z	x	y	z	D,Å
C	1	$\bar{3}$	0	0	0	0	0	0	0.00
Mn(1)	2	3	1/3	2/3	0.30314(14)	4	8	4	0.27
Mn(2)	6	1	0.33535(6)	0.16007(6)	0.30385(8)	4	2	4	0.28
Mn(3)	6	1	0.33164(6)	0.41219(6)	0.31632(10)	4	5	4	0.16
Mn(4)	6	1	0.09437(6)	0.41460(6)	0.35678(9)	1	5	4	0.26
Mn(5)	6	1	0.25044(8)	0.24126(8)	-0.00272(9)	3	3	0	0.12
As(1)	6	1	0.09897(4)	0.18907(4)	0.34454(5)	1	2	4	0.29
As(2)	6	1	0.58542(4)	0.17085(4)	0.37161(6)	7	2	4	0.34
As(3)	6	1	0.29352(4)	0.49418(4)	0.00731(6)	3	6	0	0.63
O(1)	6	1	0.2214(3)	0.2285(3)	0.2336(4)	3	3	3	0.38
O(2)	6	1	0.0231(3)	0.2427(3)	0.2397(4)	0	3	3	0.38
O(3)	6	1	0.1725(3)	0.3175(3)	0.4549(4)	2	4	5	0.43
O(4)	6	1	0.4425(3)	0.0760(3)	0.3270(4)	5	1	5	0.89
O(5)	6	1	0.5761(3)	0.1706(3)	0.5760(4)	7	2	7	0.15
O(6)	6	1	0.6540(3)	0.0881(3)	0.3750(4)	8	1	5	0.42
O(7)	6	1	0.3855(3)	0.4398(3)	0.0676(4)	4	5	1	0.63
O(8)	6	1	0.2425(3)	0.4961(3)	0.1916(4)	3	6	3	0.52
O(9)	6	1	0.1844(3)	0.3588(3)	0.9427(4)	2	4	-1	0.38
O(10)	6(×½)	1	0.1115(7)	0.0520(8)	0.0000	2	1	-1	0.98
□(1)	3	$\bar{1}$				6	0	0	
□(a)	2	3				8	4	5	
□(b)	6	1				2	1	5	
□(c)	6	1				6	6	3	
□(d)	6	1				6	3	3	
□(e)	2	3				4	8	1	
□(f)	6	1				1	5	1	
□(g)	6	1				7	2	1	
□(h)	6	1				1	2	1	
□(i)	2	3				0	0	3	

†Listed along a row are atom designation, equipoint rank number, point symmetry, atomic coordinates for refined structure, ideal (fluorite-type) atomic coordinates, and D, the displacement of real atomic positions away from fluorite-type positions in Ångström units. □(1) is the vacant cation position at ½ 0 0, etc., and □(a)•••□(i) are vacant anion positions referred to a fluorite structure.

In the final cycles of coordinate parameter refinement, the z-coordinate of O(10) was fixed at $z = 0.0$, coplanar with C as a $(CO_3)^{2-}$ group. A final Fourier map and difference synthesis revealed an essentially planar character for the $(CO_3)^{2-}$ group and clear loci of the other atomic positions (excepting hydrogen).

Full matrix refinement converged to $R = 0.072$ and $R_w = 0.056$ for all 4012 non-equivalent reflections and $R = 0.043$ for 2749 observable reflections with $|F_o| > 20$, where

$$R = \frac{\Sigma||F_o| - |F_c||}{\Sigma|F_o|}, \quad R_w = \frac{\Sigma_w(|F_o| - |F_c|)^2}{\Sigma_w F_o^2}$$

The strongest reflection was $|F_o| = 742$ for the (003) reflection.

Atomic coordinate parameters appear in Table 2, anisotropic thermal vibration parameters in Table 3, the ellipsoids of vibration in Table 4, bond distances

Table 3. Armangite: anisotropic thermal vibration parameters (×10⁴)†

Atom	β_{11}	β_{22}	β_{33}	β_{12}	β_{13}	β_{23}
Mn(1)	14.9(6)	14.9	25.9(13)	7.4	0	0
Mn(2)	17.3(4)	16.6(4)	18.7(7)	8.8(4)	0.5(4)	-0.1(4)
Mn(3)	17.8(4)	16.9(4)	50.3(9)	9.1(4)	-4.5(5)	-1.7(5)
Mn(4)	17.9(4)	16.8(4)	43.6(9)	9.5(4)	-1.9(5)	-3.5(5)
Mn(5)	16.8(5)	46.8(6)	23.8(8)	9.2(4)	0.7(5)	-1.5(6)
As(1)	15.3(3)	15.7(3)	27.4(5)	8.3(2)	1.7(3)	2.0(3)
As(2)	14.4(3)	13.9(3)	30.2(5)	6.9(2)	-1.5(3)	0.9(3)
As(3)	23.4(3)	16.3(3)	24.5(5)	8.6(2)	-0.0(3)	-1.1(3)
O(1)	14.2(19)	26.1(22)	31.4(38)	11.7(17)	1.5(22)	-1.3(24)
O(2)	15.4(20)	25.0(22)	34.6(38)	14.1(18)	-1.5(23)	-3.6(24)
O(3)	26.7(23)	24.1(22)	22.0(35)	13.6(19)	-6.9(24)	-9.9(23)
O(4)	13.3(20)	20.9(22)	54.3(46)	6.9(18)	-7.0(24)	-0.8(25)
O(5)	20.6(22)	29.0(24)	32.4(39)	11.0(19)	-3.8(24)	-8.9(25)
O(6)	15.8(21)	21.8(22)	53.6(45)	8.9(18)	0.4(25)	-8.0(26)
O(7)	26.2(25)	41.3(29)	51.0(48)	21.6(23)	-1.1(28)	5.9(30)
O(8)	27.6(24)	27.4(24)	28.6(38)	10.6(20)	4.1(25)	-3.3(24)
O(9)	19.0(21)	20.2(21)	22.6(34)	7.4(17)	-2.2(22)	-6.2(22)
C	21.4(62)	21.4	22.0(111)	10.7	0	0
O(10)	23.2(48)	32.8(56)	80.7(106)	11.3(44)	-4.8(61)	-8.8(64)

†Coefficients in the expression $\exp-[\beta_{11}h^2 + \beta_{22}k^2 + \beta_{33}\ell^2 + 2\beta_{12}hk + 2\beta_{13}h\ell + 2\beta_{23}k\ell]$. Estimated standard errors refer to the last digit except for those coefficients related by symmetry.

Table 4. Armangite: parameters for the ellipsoids of vibration†

Atom	i	u_i	θ_{ia}	θ_{ib}	θ_{ic}	$B_{equiv.}$ (Å^2)	Atom	i	u_i	θ_{ia}	θ_{ib}	θ_{ic}	$B_{equiv.}$ (Å^2)
C	1	0.094(24)	90	90	90	1.01(15)	O(1)	1	0.089(7)	164(90)	66(16)	75(21)	1.02(5)
	2	0.121(24)	···no angle determined···					2	0.112(7)	104(14)	92(13)	163(16)	
	3	0.121	···no angle determined···					3	0.135(6)	83(8)	156(38)	82(15)	
Mn(1)	1	0.101(3)	···no angle determined···			0.81(2)	O(2)	1	0.082(8)	172(90)	53(90)	86(18)	1.00(5)
	2	0.101	···no angle determined···					2	0.114(7)	96(10)	106(13)	157(16)	
	3	0.101(3)	···no angle determined···					3	0.135(6)	95(6)	139(12)	68(13)	
Mn(2)	1	0.086(2)	94(3)	87(4)	5(1)	0.80(1)	O(3)	1	0.078(8)	87(6)	69(6)	26(6)	1.13(5)
	2	0.106(1)	129(48)	10(90)	94(7)			2	0.129(6)	148(75)	31(90)	101(19)	
	3	0.110(1)	39(24)	81(15)	87(3)			3	0.142(6)	122(23)	113(17)	67(7)	
Mn(3)	1	0.105(1)	35(85)	153(90)	81(12)	1.15(1)	O(4)	1	0.090(8)	29(17)	95(9)	74(6)	1.23(5)
	2	0.108(1)	121(19)	117(22)	103(4)			2	0.125(6)	112(14)	13(90)	101(15)	
	3	0.144(1)	105(2)	88(2)	16(2)			3	0.151(6)	109(7)	78(11)	19(8)	
Mn(4)	1	0.102(1)	126(13)	13(64)	79(5)	1.07(1)	O(5)	1	0.102(7)	79(15)	71(8)	31(15)	1.28(5)
	2	0.111(1)	144(13)	94(7)	102(2)			2	0.121(6)	22(45)	106(14)	108(21)	
	3	0.134(1)	93(2)	103(2)	17(3)			3	0.153(6)	71(11)	155(26)	66(9)	
Mn(5)	1	0.097(2)	100(5)	88(1)	10(5)	1.57(1)	O(6)	1	0.103(7)	165(90)	71(41)	80(23)	1.26(5)
	2	0.108(1)	149(2)	89(1)	100(6)			2	0.114(7)	85(29)	144(38)	118(16)	
	3	0.196(1)	61(6)	177(90)	88(1)			3	0.156(6)	76(6)	120(8)	30(8)	
As(1)	1	0.099(1)	106(55)	114(54)	44(20)	0.84(1)	O(7)	1	0.113(7)	21(60)	124(19)	70(18)	1.65(6)
	2	0.100(1)	157(90)	37(90)	91(42)			2	0.142(7)	69(11)	86(10)	152(11)	
	3	0.110(1)	74(4)	64(4)	46(4)			3	0.172(6)	90(6)	35(9)	72(10)	
As(2)	1	0.097(1)	52(39)	154(73)	67(18)	0.83(1)	O(8)	1	0.101(7)	105(7)	77(7)	17(7)	1.38(6)
	2	0.099(1)	132(17)	106(22)	101(8)			2	0.133(6)	118(77)	122(89)	91(7)	
	3	0.112(1)	114(3)	70(3)	26(4)			3	0.156(6)	33(50)	145(46)	73(13)	
As(3)	1	0.098(1)	93(1)	71(4)	20(4)	1.01(1)	O(9)	1	0.086(8)	86(9)	69(7)	28(12)	1.01(5)
	2	0.107(1)	92(2)	34(3)	110(5)			2	0.115(6)	44(23)	81(14)	111(10)	
	3	0.132(1)	4(90)	117(10)	88(2)			3	0.133(6)	46(37)	157(90)	73(18)	
							O(10)	1	0.125(13)	37(42)	84(19)	80(10)	1.93(13)
								2	0.154(13)	53(38)	157(87)	111(33)	
								3	0.185(12)	85(14)	112(20)	24(13)	

†i = ith principal axis, u_i = rms amplitude, θ_{ia}, θ_{ib}, θ_{ic} = angles (deg.) between the ith principal axis and the cell axes a_1, a_2 and c. The equivalent isotropic thermal parameter, B, is also listed. Estimated standard errors in parentheses refer to the last digit.

and angles in Table 5, electrostatic valence balances in Table 6, and a list of the structure factors in Table 7.[1]

Description of the structure

Armangite is derived from the fluorite structure type by the ordering of vacancies over the anion frame. The a_1-axis is parallel to the [110] direction of the fluorite cell, with a_1 (arm) = $2\sqrt{2}\ a_1$ (flu). Thus, the fluorite cell edge would be 4.77A in this direction. The c-axis is parallel to the [111] direction of the fluorite cell, with c (arm) = $\sqrt{3}\ a_1$ (flu), corresponding to a 5.11A fluorite edge. The average of 4.94A agrees well with 4.92A found in the structurally-related cubic magnussonite (Moore and Araki, 1979), where a_1 (mag) = $4a_1$ (flu).

The armangite cell thus contains 12 fluorite cells with a stoichiometry $X_{48}\phi_{96}$, where the X's are the cation positions and the ϕ's are the anion positions in the fluorite frame. For armangite 48X = $26Mn^{2+}$ + $18As^{3+}$ + $1(CO_3)$ + $3\square(1)$, the cation vacancies occurring at ½ ½ 0, *etc.*, and 96ϕ = 54[O(1)–O(9)] + 42[□(a)–□(i)]. The distributions of cations, anions and vacancies are listed in Table 2. The fluorite frame defines the ideal positions of cations, anions and vacancies for x and y must be ±m/12; and z must be ±4n/12 for cations and ±(2p+1)/12 for anions, where m, n, and p are integers. In Table 2, the calculated deviations from ideal fluorite positions range from 0.00 for C to 0.89A for O(4), with a mean 0.36A displacement away from perfect fluorite positions. Therefore the ideal distributions of holes and vacancy types over the cubic domain can be defined.

[1]To obtain a copy of Table 7, order Document AM-79-105 from the Business Office, Mineralogical Society of America, 2000 Florida Ave. NW, Washington, DC 20009. Please remit $1.00 in advance for the microfiche.

Table 5. Armangite: bond distances and angles†

Mn(1)			**Mn(3)**		
3 Mn(1)-O(5)$^{(1)}$	2.185(4)		1 Mn(3)-O(6)$^{(2)}$	2.052(4)	
3 Mn(1)-O(8)	2.226(4)		1 Mn(3)-O(5)$^{(5)}$	2.142(4)	
average	2.206		1 Mn(3)-O(3)	2.237(4)	
		Angles (°)	1 Mn(3)-O(1)	2.282(4)	
3 O(5)$^{(4)}$-O(8)	2.804(5)*	78.9(1) c	1 Mn(3)-O(7)	2.291(4)	
3 O(5)$^{(5)}$-O(8)	2.868(5)*	81.1(1) c	1 Mn(3)-O(8)	2.305(4)	
3 O(5)$^{(1)}$-O(5)$^{(5)}$	3.300(6)	98.1(1) d	average	2.218	
3 O(8)-O(8)$^{(2)}$	3.454(6)	101.8(1) d			
average	3.107	90.0	1 O(1)-O(3)	2.552(5)**	68.7(1) c
			1 O(7)-O(8)	2.640(5)**	70.1(1) c
As(1)			1 O(1)-O(6)$^{(2)}$	2.786(5)*	79.8(1) c
			1 O(5)$^{(5)}$-O(8)	2.804(5)*	78.1(1) c
1 As(1)-O(1)	1.760(3)		1 O(1)-O(7)	2.980(5)*	81.4(1) c
1 As(1)-O(2)	1.782(3)		1 O(3)-O(8)	3.140(5)	87.5(1) c
1 As(1)-O(3)	1.795(3)		1 O(6)$^{(2)}$-O(7)	3.205(5)	95.0(1) d
average	1.779		1 O(3)-O(5)$^{(5)}$	3.341(5)	99.4(1) d
			1 O(5)$^{(5)}$-O(6)$^{(2)}$	3.343(5)	105.7(1) d
1 O(1)-O(3)	2.552(5)**	91.7(2) c	1 O(3)-O(6)$^{(2)}$	3.427(5)	106.0(1) d
1 O(2)-O(3)	2.584(5)**	92.5(2) c	1 O(1)-O(8)	3.497(5)	99.4(1) d
1 O(1)-O(2)	2.777(5)	103.3(2) d	1 O(5)$^{(5)}$-O(7)	3.594(5)	108.3(1) d
average	2.638	95.8	average	3.109	90.0
As(2)			**Mn(4)**		
1 As(2)-O(4)	1.745(3)		1 Mn(4)-O(4)$^{(3)}$	2.069(4)	
1 As(2)-O(6)	1.772(3)		1 Mn(4)-O(5)$^{(4)}$	2.193(4)	
1 As(2)-O(5)	1.814(4)		1 Mn(4)-O(3)	2.228(4)	
average	1.777		1 Mn(4)-O(2)	2.268(4)	
			1 Mn(4)-O(8)	2.268(4)	
1 O(5)-O(6)	2.585(5)**	92.3(2) c	1 Mn(4)-O(6)$^{(4)}$	2.396(4)	
1 O(4)-O(5)	2.727(5)	100.0(2) c	average	2.237	
1 O(4)-O(6)	2.808(5)	106.0(2) d			
average	2.707	99.4	1 O(2)-O(3)	2.584(5)**	70.1(1) c
			1 O(5)$^{(4)}$-O(6)$^{(4)}$	2.585(5)**	68.4(1) c
As(3)			1 O(2)-O(4)$^{(3)}$	2.721(5)*	77.6(1) p,c
			1 O(3)-O(6)$^{(4)}$	2.798(5)*	114.4(1) p,c
1 As(3)-O(9)	1.773(3)		1 O(5)$^{(4)}$-O(8)	2.868(5)*	80.0(1) p,c
1 As(3)-O(8)	1.776(4)		1 O(3)-O(8)	3.140(5)*	88.6(1) c
1 As(3)-O(7)	1.809(4)		1 O(2)-O(8)	3.242(5)	91.2(1) d
average	1.786		1 O(4)$^{(3)}$-O(6)$^{(4)}$	3.267(5)	93.8(1) c
			1 O(4)$^{(3)}$-O(5)$^{(4)}$	3.322(5)	102.4(1) d
1 O(7)-O(9)	2.610(5)**	93.6(2) c	average	2.947	82.9
1 O(7)-O(8)	2.640(5)**	94.8(2) c			
1 O(8)-O(9)	2.730(5)	100.6(2) d	prism diagonals		
average	2.660	96.3		Angles (°)	
			O(3)-O(5)$^{(4)}$	116.6(1)	
C			O(2)-O(6)$^{(4)}$	123.0(1)	
			O(4)$^{(3)}$-O(8)	129.9(1)	
3 C-O(10)	1.303(8)		O(3)-O(4)$^{(3)}$	130.0(1)	
3 O(10)-O(10)$^{(2)}$	2.257(13)	120.0	O(6)$^{(4)}$-O(8)	131.1(1)	
			O(2)-O(5)$^{(4)}$	168.6(1)	
			average	133.2	
Mn(2)			**Mn(5)**		
1 Mn(2)-O(3)$^{(4)}$	2.148(3)		1 Mn(5)-O(2)$^{(4)}$	2.114(4)	
1 Mn(2)-O(9)$^{(4)}$	2.200(3)		1 Mn(5)-O(1)	2.120(4)	
1 Mn(2)-O(2)$^{(2)}$	2.238(3)		1 Mn(5)-O(9)$^{(4)}$	2.133(3)	
1 Mn(2)-O(1)	2.241(3)		1 Mn(5)-O(9)	2.226(4)	
1 Mn(2)-O(4)	2.250(4)		1 Mn(5)-O(10)	2.291(9)	
1 Mn(2)-O(6)$^{(2)}$	2.263(3)		1 Mn(5)-O(7)	2.450(4)	
average	2.223		average	2.222	
1 O(2)$^{(2)}$-O(4)	2.721(5)*	74.7(1) c	x 1 Mn(5)$^{(4)}$-O(10)	2.280(9)	
1 O(1)-O(9)$^{(4)}$	2.785(5)*	77.7(1) c			
1 O(1)-O(6)$^{(2)}$	2.786(5)*	76.4(1) c	1 O(7)-O(9)	2.610(5)**	67.7(1) c
1 O(3)$^{(4)}$-O(6)$^{(2)}$	2.798(5)*	78.7(1) c	1 O(1)-O(9)$^{(4)}$	2.785(5)*	81.8(1) c
1 O(2)$^{(2)}$-O(9)$^{(4)}$	2.869(5)*	80.5(1) c	1 O(2)$^{(4)}$-O(9)	2.869(5)*	82.7(1) c
1 O(3)$^{(4)}$-O(4)	3.003(5)*	86.1(1) c	1 O(9)$^{(4)}$-O(10)	2.934(8)*	81.3(2) d
1 O(4)-O(9)$^{(4)}$	3.200(5)	92.0(1) d	x 1 O(1)-O(10)	2.935(7)	83.3(1) c
1 O(2)$^{(2)}$-O(3)$^{(4)}$	3.347(5)	99.5(1) d	x 1 O(2)$^{(4)}$-O(10)	2.958(7)	84.3(1) d
1 O(1)-O(2)$^{(2)}$	3.382(5)	98.1(1) d	1 O(1)-O(7)	2.980(5)*	81.0(1) c
1 O(6)$^{(2)}$-O(9)$^{(4)}$	3.457(5)	101.5(1) d	1 O(2)$^{(4)}$-O(9)$^{(4)}$	3.271(5)	100.7(1) d
1 O(1)-O(3)$^{(4)}$	3.466(5)	104.3(1) d	1 O(1)-O(9)	3.294(5)	98.6(1) d
1 O(4)-O(6)$^{(2)}$	3.726(5)	111.3(1) d	1 O(7)-O(9)$^{(4)}$	3.416(5)	96.1(1) d
average	3.128	90.1	1 O(2)$^{(4)}$-O(7)	3.771(4)	111.2(1) d
			x 1 O(9)-O(10)	3.778(7)	113.6(1) c
			average	3.133	90.2
			x 1 O(1)$^{(4)}$-O(10)	2.845(7)	80.5(1)
			x 1 O(9)-O(10)$^{(5)}$	2.934(8)	83.0(2)
			x 1 O(2)$^{(2)}$-O(10)	3.024(7)	86.9(1)
			x 1 O(9)$^{(2)}$-O(10)	3.723(10)	115.0(2)
			average	3.132	91.3

†Estimated standard errors in parentheses refer to the last digit. The equivalent positions (referred to Table 2) are designated as superscripts and are (1) = -x, -y, -z; (2) = y-x, -x, z; (3) = -y, x-y, z; (4) = y, y-x, -z; and (5) = x-y, x, -z.

*O–O′ edge shared between Mn–O polyhedra. **O–O′ edge shared between Mn–O and As–O polyhedra.

[c]Edges referred to the cubic domain. [d]Face diagonals referred to the cubic domain. [p]Edges of the pseudo-trigonal prism.

[x]Edges which are affected by half-occupied (disordered) O(10). The first O–O′ average obtains from the polyhedron labelled in Fig. 2a. The second O–O′ from substitution of the alternative edge distances.

Table 6. Armangite: electrostatic valence balance of cations and anions†

	Coordinating Cations									Δp_O	Bond Length Deviations							
	C	Mn(1)	Mn(2)	Mn(3)	Mn(4)	Mn(5)	As(1)	As(2)	As(3)		Mn(1)	Mn(2)	Mn(3)	Mn(4)	Mn(5)	As(1)	As(2)	As(3)
Anions																		
O(1)	-	-	1	1	-	1	1	-	-	0.00	-----	+0.02	+0.06	-----	-0.10	-0.02	-----	-----
O(2)	-	-	1	-	1	1	1	-	-	0.00	-----	+0.01	-----	+0.03	-0.11	+0.00	-----	-----
O(3)	-	-	1	1	1	-	1	-	-	0.00	-----	-0.07	+0.02	-0.01	-----	+0.02	-----	-----
[a]O(4)	-	-	1	(1)	1	-	-	1	-	(0.00) -0.33	-----	+0.03	-----	-0.17	-----	-----	-0.03	-----
O(5)	-	1	-	1	1	-	-	1	-	0.00	-0.02	-----	-0.08	-0.04	-----	-----	+0.04	-----
O(6)	-	-	1	1	1	-	-	1	-	0.00	-----	+0.04	-0.17	+0.16	-----	-----	-0.01	-----
[b]O(7)	-	-	-	1	-	1	-	-	1	-0.33	-----	-----	+0.07	-----	+0.23	-----	-----	+0.02
O(8)	-	1	-	1	1	-	-	-	1	0.00	+0.02	-----	+0.09	+0.03	-----	-----	-----	-0.01
O(9)	-	-	1	-	-	2	-	-	1	0.00	-----	-0.02	-----	-----	+0.00, -0.09	-----	-----	-0.01
O(10)	1	-	-	-	-	1 (2)	-	-	-	-0.33 (0.00)	-----	-----	-----	-----	+0.07	-----	-----	-----

†A bond length deviation refers to the polyhedral average subtracted from the individual bond distance, Δp_O = deviation of electrostatic bond strength sum from neutrality (p_O = 2.00 e.s.u.).

[a]Probably does not receive a bond from Mn(3) since Mn(3)–O(4) = 3.19 Å.

[b]Most likely O(7) = $OH_{2/3}O_{1/3}$.

In Figures 1a and 1b these idealized arrangements are shown for the two unique levels at $z = 0$ and 1/3. The vacancy types are thus Mn(1) = $u^6d^2(3)$, ($\bar{3}$ 2/m:3); Mn(2) = $u^6d^2(3)$, ($\bar{3}$ 2/m:1); Mn(3) = $u^6d^2(2)$, (2mm:1); Mn(4) = $u^6d^2(1)$, (2mm:1); Mn(5) = $u^5d^3(2)$, (m:1); As(1) = As(2) = As(3) = $u^3d^5(1)$, (m:1). Here the nomenclature adopts the procedure of earlier studies (Moore and Araki, 1976b; 1977; 1979): the vacancy types are listed followed by their (maximal symmetry: symmetry in the crystal). The Mn(5)–O polyhedron receives an additional oxygen not belonging to the fluorite frame, namely O(10) which is associated with $(CO_3)^{2-}$, and is therefore six-coordinate in the crystal. The $(CO_3)^{2-}$ group is an aggregate centered on an open cavity and plays a role much like ClW in the magnussonite structure (Moore and Araki, 1979). Thus, armangite is an unusually elegant and complex version of the fluorite family of derivative structures. The stability of the ionic part of the structure is doubtless a result of the inherent stability of the fluorite structure type.

Figures 2a and 2b feature the structure design as polyhedral diagrams for the two non-equivalent levels at $z = 0$ and 1/3. Mn(1), Mn(2), and Mn(3) are distorted octahedra; Mn(4) is a distorted trigonal prism; As(1), As(2), and As(3) are distorted trigonal pyramids (see Moore and Araki, 1979). The discussion above facilitates easy description of the polyhedral bond distances and angles listed in Table 5. Shared edges correspond to those edges of the cubic domain which remain after vertices are appropriately vacated. The unshared edges are those edges which

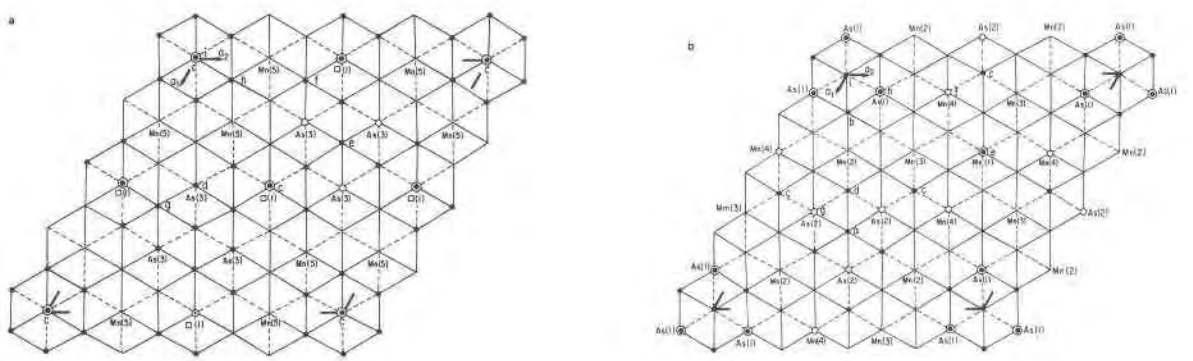

Fig. 1. Idealized fluorite checkerboards of the independent levels at $z = 0$ (Fig. 1a) and $z = 1/3$ (Fig. 1b). These correspond to the fluorite-type arrangement down [111]. Solid disks are meridional vacancies or vacancies above the plane, open disks are vacancies below the plane. □(1), a cation vacancy and the labelled cation positions refer to Table 2 as do the non-equivalent anion vacancies labelled a to i. C at the origin refers to the carbon atom position.

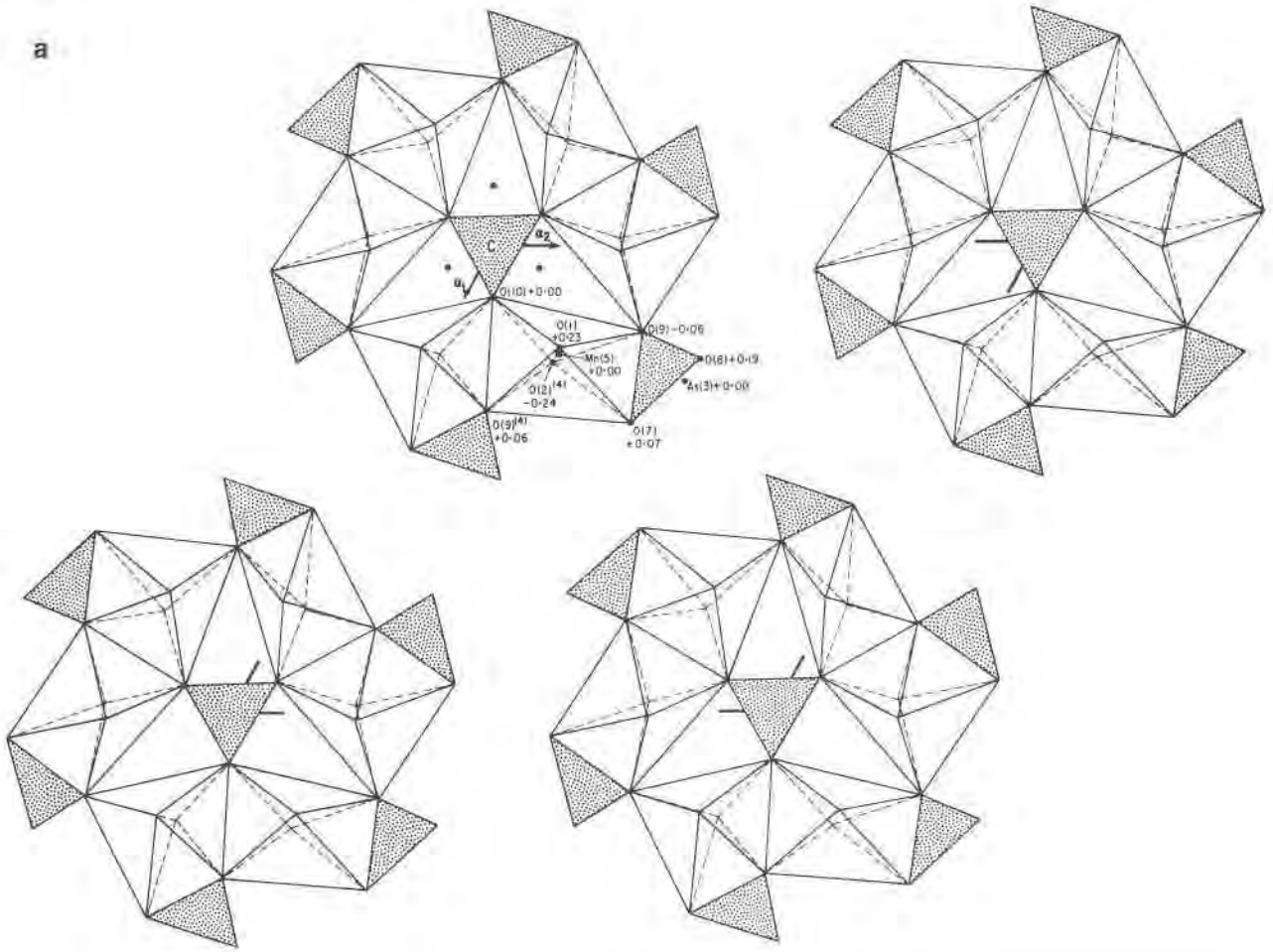

Fig. 2a. Polyhedral representation of the level at $z = 0$. The atom positions are labelled to conform with Table 2 and Table 5. An ordered arrangement with point symmetry C_3 is shown. The triangle of dots refers to the alternative positions of O(10), which is half-populated on the average. Heights are given as fractional coordinates in z.

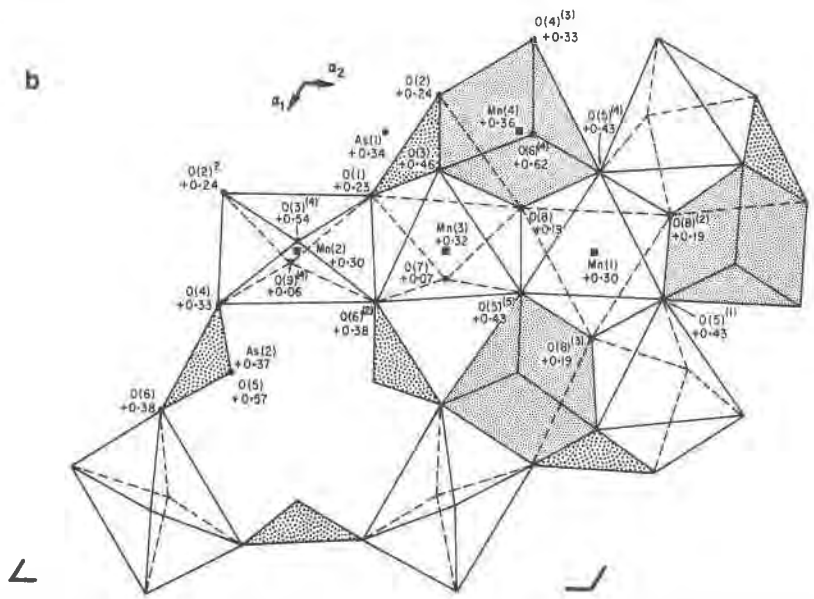

Fig. 2b. Polyhedral representation of the level at $z = 1/3$. The $Mn(4)O_6$ trigonal prisms are finely stippled, and the trigonal pyramidal arsenite oxygens are coarsely stippled. The atom positions are labelled to conform with Table 2 and Table 5. Heights are given as fractional coordinates in z.

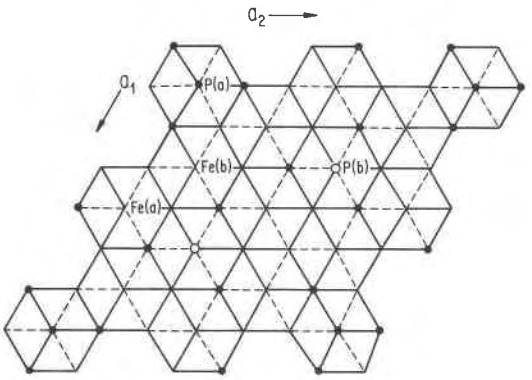

Fig. 3. The Fe^{2+} oxyphosphate sheet in mitridatite represented as an idealized fluorite checkerboard. See Figs. 1a and 1b.

are obtained from distortions away from the cube and from lower coordination number. These correspond to face diagonals of the cubic domain and are nearly always longer than the shared edges because of electrostatic repulsion of cations across shared edges. Exceptions, where some cube edges are longer than face diagonals, occur in O–O(10) distances, but here the O(10) anion is removed 0.98A from the perfect fluorite arrangement, which is further reason why (CO_3) is treated as an aggregate. It is further seen (Table 5) that the armangite structure possesses polyhedral distortions expected for an ionic crystal, and therefore we shall discuss these in more detail.

Bond distances and angles

Setting coordination numbers as bracketed superscripts, the polyhedral interatomic averages are: $^{[3]}$As(1)–O 1.78, $^{[3]}$As(2)–O 1.78, $^{[3]}$As(3)–O 1.79, $^{[6]}$Mn(1)–O 2.21, $^{[6]}$Mn(2)–O 2.22, $^{[6]}$Mn(3)–O 2.22, $^{[6]}$Mn(4)–O 2.24, and $^{[6]}$Mn(5)–O 2.22A. As seen in Figure 2a, $Mn(5)O_6$ is split into two distorted octahedra owing to disordered O(10), but their Mn(5)–O averages are practically the same since Mn(5)–O(10) = 2.29A and $Mn(5)^{(4)}$–O(10) = 2.28A. Since the $(CO_3)^{2-}$ triangles are rotationally disordered (the static model would have C_3 symmetry), the $Mn(5)O_6$ octahedra are also disordered because of an average half-occupancy of O(10) in a general position. The equivalent isotropic thermal vibration parameters (B in A^2 units) range from 0.83 to 1.01 for As, 1.0 for C, 0.80 to 1.57 for Mn and 1.00 to 1.93 for the oxygens. The Mn(5) and O(10) thermal parameters are the largest for the atom positions, which is probably a consequence of disordered O(10). Taken together, distances and thermal parameters indicate a crystal with fully-occupied sites, excepting half-occupied O(10), and formal charges of As = As^{3+}, C = C^{4+}, and Mn = Mn^{2+}. Bond strength sums, Table 6, allow assignment of formal charges on the oxygens; we used the bond length–bond strength procedure outlined by Baur (1970). For a fluorite derivative structure, anions must each be four-coordinated by the cations. One cation position, (1) at ½ ½ 0, *etc.*, is empty, however, and we see that O(7) is only three-coordinated by populated cation sites and that all individual distances are longer than average although the anion is *undersaturated* with respect to cations. Therefore, O(7) must be coordinated by a proton as well, and we propose that the proton site is on the average 2/3-occupied. The remaining anions show a bond distance distribution consistent with oxide anions.

We believe the formula for armangite can be rather precisely written, that is:

$$Mn_{26}^{2+}[As_6^{3+}(OH)_4O_{14}][As_6^{3+}O_{18}]_2[CO_3]$$

The (CO_3) polyhedron

The CO_3 equilateral triangle is situated at the origin of the cell and resides in the center of a fluorite-type cation position whose eight cubic anion vertices are all empty (Fig. 1a). Thus the entire CO_3 group is accepted as an aggregate in a fluorite-type cation position, the oxide *not* belonging to the fluorite-type framework even though O(10) does not deviate greatly from a fluorite position (see Fig. 2a and Table 2, where D = 0.98A), although its position is at $z = 0$ whereas in the fluorite arrangement, $z \sim +1/12$ or $-1/12$. One ordered arrangement requires that the local point symmetry is C_3, not C_{3i}. However, this orientation is statistically half-occupied on the average, the alternative inverted orientation effecting a rotation of 60° about the *c*-axis. This merely reorients O(10) but leaves the topology of the rest of the structure unchanged.

The C–O distance of 1.30A is within the error of C–O = 1.27–1.29A distances found for simple carbonates (De Villiers, 1971). Armangite is the first arsenite–carbonate reported ever.

The $Mn(5)O_6$ polyhedron

The O(10) oxygen, also associated with the $(CO_3)^{2-}$ group, leads to a local cluster at $z = 0$ which consists of six $As(3)O_3$ trigonal pyramids, six $Mn(5)O_6$ octahedra and a central CO_3 group, leading to a cluster composition of $Mn_6^{2+}As_6^{3+}C^{4+}O_{33}$. In many respects, it is topologically similar to a cluster component in the

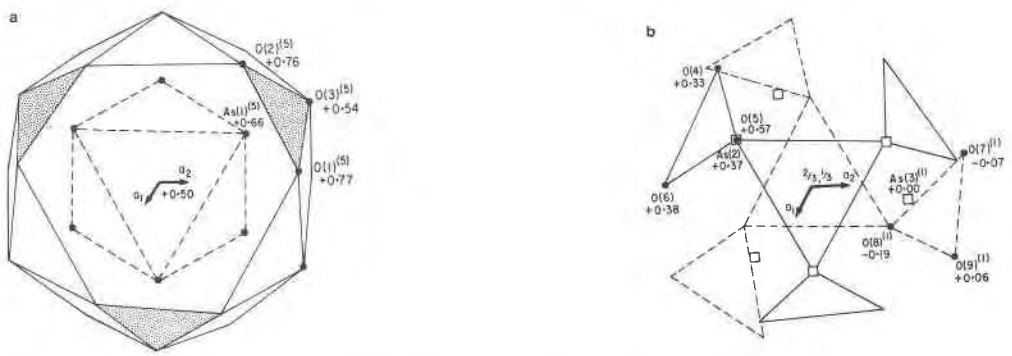

Fig. 4. (a) Oxygen environment around the As(1) atoms which define a distorted octahedron centered at $z = 0.5$. The outer polyhedron consists of 18 vertices corresponding to O(1), O(2), and O(3), 2 hexagonal faces, 12 triangular faces and 6 quadrilateral faces of point symmetry C_{3i}. This arrangement is similar to the one found in magnussonite. (b) Oxygen environment around the As(2) and As(3) atoms, centered at 2/3 1/3 ~0.19. The central As atoms also define a distorted octahedron, and the oxygens define a distorted cuboctahedron with point symmetry C_3.

Fe^{3+} oxyphosphate sheet of the complex mitridatite structure (Moore and Araki, 1977). In fact, the mitridatite sheet itself can be extracted from ordered anion vacancies over fluorite cubes and is therefore a sheet which is a fluorite derivative (Fig. 3). Placement of the additional $CaO_5(H_2O)_2$ polyhedra above and below the sheet, each polyhedron sharing three edges with the FeO_6 octahedra, also satisfy a fluorite arrangement, but the relationship breaks down further away since the polyhedra link by edge-sharing to form $Ca_2O_{10}(H_2O)_2$ dimers along a common (H_2O)–(H_2O) edge, a juncture which is not isomorphic to the fluorite-type arrangement.

Relationship to magnussonite

Armangite and magnussonite are closely related chemically, but the compounds are not dimorphic since magnussonite possesses no $(CO_3)^{2-}$ groups and armangite possesses no Cl^-. Both are derived from the fluorite structure, and the fraction of anion vacancies are very similar. Magnussonite possesses cubic, trigonal prismatic, distorted square pyramidal, and distorted octahedral coordinations about Mn^{2+} (Moore and Araki, 1979), while armangite possesses only distorted octahedral and trigonal prismatic coordinations about Mn^{2+}.

Perhaps the most interesting feature in the two structures is an oxygen polyhedron consisting of 36 edges, 18 vertices, 2 hexagonal faces, 12 triangular faces, and 6 quadrilateral faces of point symmetry C_{3i}. An identical polyhedron also of point symmetry $\bar{3}$ occurs in armangite at 0 0 ½ (Fig. 4a) and surrounds a "core" of six $As(1)^{3+}$ which define a distorted octahedron with a mean edge distance of 3.68A compared with 3.73A in magnussonite. Although in magnussonite the center is occupied by Mn^+ defining an As_6Mn metallic cluster (which satisfies the 18-electron rule), search for a residue on a difference synthesis for armangite failed to locate any residue beyond two electrons/A^3. In addition, As(2) and As(3) also define an octahedral "core" in armangite with mean edge distance As–As = 3.54A (Fig. 4b). But the oxygen polyhedron is quite different, being a distorted cuboctahedron with point symmetry C_3. Again, difference synthesis failed to reveal any occupancy at the center, at 2/3 1/3 ~0.19.

Why does magnussonite exhibit inferred Mn^+ in the center which could not be located in the structurally-related armangite? Is it possible that cumulative errors in absorption correction led to a false peak at 0 0 0 in the magnussonite structure? Since a peak was found in both crystals of magnussonite studied but not in the special positions of armangite, errors in absorption correction are unlikely to be of much significance. It can also be argued that an absorption error (or lack of absorption correction) would more likely lead to a negative difference at the origin since $|F_o| < |F_c|$ would be prominent at low angles. The ratio of equipoint rank number for the C_{3i} positions to general positions is 1:6 in both compounds. Since the linear atomic absorption coefficients of both compounds are similar, we believe the structural differences between the two compounds to be real. It is likely that the fields of stability for armangite and magnussonite are sufficiently different that the As_6Mn metallic cluster may be stable in one but not the other.

Acknowledgments

We appreciate a portion of the sample U71 from the Mineralogical Section, Swedish Natural History Museum and a portion of

sample R5795 from Mr. John S. White, Jr. of the Department of Mineral Sciences, National Museum of Natural History (Smithsonian Institution). We thank Mr. Todd Solberg for the probe analysis of carbon in armangite. This work was supported by NSF grant EAR-75-19483.

References

Aminoff, G. and R. Mauzelius (1920) Armangite, a new arsenite from Langbanshyttan. *Geol. Fören. Förhandl., 42,* 301–309.

Araki, T. (1977) A structure factor L.S. refinement program for reflection data with a twinned crystal. *Am. Crystallogr. Assoc. Summer Meeting Program and Abstracts, 5 no. 2,* 68.

Baur, W. H. (1970) Bond length variation and distorted coordination polyhedra in inorganic crystals. *Trans. Am. Crystallogr. Assoc., 6,* 129–155.

Burnham, C. W. (1966) Computation of absorption corrections, and the significance of the end effect. *Am. Mineral., 51,* 159–167.

De Villiers, J. P. R. (1971) Crystal structures of aragonite, strontianite, and witherite. *Am. Mineral., 56,* 758–767.

Ibers, J. A. and W. C. Hamilton (Eds.) (1974) *International Tables for X-ray Crystallography, Vol. IV.* Kynoch Press, Birmingham, England.

Moore, P. B. and T. Araki (1976a) A mixed-valence solid-solution series: crystal structures of phosphoferrite and kryzhanovskite. *Inorg. Chem., 15,* 316–321.

——— and ——— (1976b) Braunite: its structure and relationship to bixbyite, and some insights on the genealogy of fluorite derivative structures. *Am. Mineral., 61,* 1226–1240.

——— and ——— (1977) Parwelite, a complex anion-deficient fluorite derivative structure. *Inorg. Chem., 16,* 1839–1847.

——— and ——— (1979) Magnussonite, a fluorite derivative structure. *Am. Mineral., 64,* 390–401.

Palache, C., H. Berman and C. Frondel (1960) *The System of Mineralogy of Dana, Vol. 2 (7th ed.).* Wiley, New York, pp. 1031–1032.

Manuscript received, July 27, 1978;
accepted for publication, February 16, 1979.